HIV-1 Vpr disrupts mitochondria axonal transport and accelerates neuronal aging

Ying Wang[1,¶], **Maryline Santerre**[1], **Italo Tempera**[2], **Kayla Martin**[1], **Ruma Mukerjee**[1], and **Bassel E Sawaya**[1,3,¶]

[1]Molecular Studies of Neurodegenerative Diseases Lab

[2]The Fels Institute for Cancer Research & Molecular Biology, [2]Department of Neurology

[3]Temple University School of Medicine, Philadelphia, PA 19140

Abstract

Disruption of mitochondria axonal transport, essential for the maintenance of synaptic and neuronal integrity and function, has been identified in neurodegenerative diseases. Whether HIV-1 viral proteins affect mitochondria axonal transport is unknown, albeit HIV-associated neurocognitive disorders occur in around half of the patients living with HIV. Therefore, we sought to examine the effect of HIV-1 viral protein R (Vpr) on mitochondria axonal transport. Using mice primary neuronal cultures, we demonstrated that 4-day Vpr treatment reduced the ratio of moving mitochondria associated with (i) less energy (ATP) supply, (ii) reduction in Miro-1 and (iii) increase of α-synuclein which led to loss of microtubule stability as demonstrated by inconsecutive distribution of acetylated α-tubulin along the axons. Interestingly, the effect of Vpr on mitochondria axonal transport was partially restored in the presence of bongkrekic acid, a compound that negatively affected the Vpr-adenine nucleotide translocator (ANT) interaction and totally restored the ATP level in neurons. This indicated Vpr impaired mitochondria axonal transport partially related to its interaction with ANT. The above effect of Vpr was similar to the data obtained from hippocampal tissues isolated from 18-month-old aging mice compared to 5-month-old mice. In accord with previous clinical findings that HIV infection prematurely ages the brain and increases the susceptibility to HAND, we found that Vpr induced aging markers in neurons. Thus, we concluded that instead of causing cell death, low concentration of HIV-1 Vpr

¶Corresponding Author: Bassel E Sawaya, PhD, Molecular Studies of Neurodegenerative Diseases Lab, Department of Neurology & The Fels Institute for Cancer Research & Molecular Biology, Temple University School of Medicine, 3307 North Broad Street, PHAB # 302, Philadelphia, PA 19140, Phone: 215-707-5446, Fax: 215-707-5948, sawaya@temple.edu. Ying Wang, PhD, The Fels Institute for Cancer Research & Molecular Biology, Temple University School of Medicine, 3307 North Broad Street, PHAB # 302, Philadelphia, PA 19140, Phone: 267-886-6616, wangying8305@gmail.com.

Competing interests

The authors declared that they have no competing interests.

altered neuronal function related with inhibition of mitochondria axonal transport which might contribute to the accelerated neuronal aging.

Keywords

INTRODUCTION

The combined anti-retroviral therapy (cART) has been extremely effective in suppressing viral replication and extending the life expectancy of HIV-infected patients. However, neuropsychological studies revealed a significant number of HIV-1 infected patients developing neurocognitive impairment despite of reduced morbidity and mortality by the treatment. These impairments include learning deficit, declarative memory and executive function alterations (Borjabad et al., 2011; Fellows et al., 2014; Heaton et al., 2011). HIV viral proteins are believed to contribute to the development of HIV-associated neurocognitive disorder (HAND). This was confirmed in transgenic rodents expressing one of the HIV viral proteins that exhibited learning and memory deficits (Carey et al., 2012; D'Hooge et al., 1999; Jones et al., 2007). Therefore, understanding how HIV viral proteins contribute to learning and memory deficits is critical for reducing the neurocognitive impairment in HIV patients.

The virion-associated HIV-1 viral protein R (Vpr) is a multi-potent viral protein involved in nuclear import of the viral pre-integration complex, inducing G2-phase arrest and the regulation of HIV-LTR activation (Bartz et al., 1996; Forget et al., 1998; He et al., 1995; Jenkins et al., 1998). Recently, Vpr was shown to facilitate viral replication in the host cells by mediating proteasomal degradation of host restriction factors (Laguette et al., 2014; Zhou et al., 2015). Using different cell lines with neuronal features, studies showed that Vpr induces apoptosis, impairs mitochondrial function and axonal outgrowth, eventually leading to neuronal loss together with learning and memory deficit in Vpr-transgenic mice (Jones et al., 2007; Kitayama et al., 2008). Most of these studies proposed neuronal apoptosis as the mechanism contributing to the neurocognitive impairment (Cheng et al., 2007; Guha et al., 2012). However, in the cART era, milder forms of neurocognitive impairment dominate, in which neuronal death is not commonly seen as in cases of HIV-associated dementia which dominated in the pre-cART era (Heikinheimo et al., 2015). Therefore, identifying non-apoptotic mechanisms would help to control the progression of HAND.

Axonal transport is crucial for the maintenance of neuronal metabolism and synaptic transmission, therefore indispensable for the survival and function of neurons (Bartlett et al., 1998; Chevalier-Larsen and Holzbaur, 2006; Maday et al., 2014). Normal function and dynamic of mitochondria, the "powerhouse of the cell" and "ATP reservoir", are critical for the neuronal cells with tremendous energy demands. Mitochondria axonal transport distributes refreshed, healthy mitochondria from the cell body to the synaptic terminals and transports older, damaged mitochondria from the axonal terminal to the soma (Frederick and Shaw, 2007). This energy-consuming process depends on ATP hydrolysis and requires the

interaction between adaptor proteins, motor complexes and stable microtubule system (Schwarz, 2013). Axonal transport disruption can trigger synaptic accumulation of autophagosomes packed with damaged mitochondria and protein aggregates, promoting synaptic failure (Esteves et al., 2014). Aberrant axonal transport was observed in several neurodegenerative diseases such as Parkinson's disease (PD) and Lewy's body dementia (LBD), both of which have aberrant α-synuclein accumulation (Lamberts et al., 2015; O'Donnell et al., 2014; Volpicelli-Daley et al., 2014).

Recently, α-synuclein was found to affect vesicle transport in CNS neurons (Koch et al., 2015). Another group found α-synuclein accumulation did not cause a generalized defect in axonal transport but impaired the transport of Rab7 and TrkB receptor-containing endosomes and autophagosomes (Volpicelli-Daley et al., 2014). These studies indicated α-synuclein might be a negative regulator of axonal transport and targeting the early effect of α-synuclein accumulation like axonal transport deficiency may be a novel intervention against neurocognitive disorder.

In here, we aim to (i) determine whether Vpr affects mitochondria axonal transport; and to (ii) explore the mechanisms underlying the phenotype changes in primary neurons treated with low concentration of Vpr.

1.1. Cell culture, transfection and treatment

Primary neuronal cultures were prepared as previously described with minor modifications. Briefly, hippocampus were collected from embryonic mice of 17–18 days old (C57/BL6 mice, Taconic farm), digested in 0.125% trypsin for 30 minutes and then rinsed twice in HBSS solution (Corning cellgro). Digested tissue was then triturated and dissociated into single cells in seeding medium (DMEM containing 4.5 g/L glucose, 10% FBS, $1 \times$ glutamax, $1 \times$ non-essential amino acids, 100 IU/ml penicillin and streptomycin, Invitrogen). Cells in suspension were centrifuged at 150 g for 10 minutes and the pellet was gently re-suspended in the seeding medium. The pellet was passed through mesh #400 to remove the non-dispersed tissue before seeded to plates.

Human embryonic kidney cells (HEK293) were bought from American Type Culture Collection (ATCC) and kept in DMEM (4.5 g/L glucose, Corning cellgro) medium with 10% FBS (Gibco). SH-SY5Y cells were bought from ATCC and kept in DMEM/F12 medium (Corning cellgro) with 10% FBS. Forty-eight hours after plating, 10 μM retinoic acid (Sigma-aldrich) was added to SH-SY5Y cells and allowed for differentiation for 3 days before collection.

1.2. Transfection and luciferase assay

For transfection, 4×10^6 cells (mice primary neurons) were re-suspended in Lonza P3 medium (Cat # V4XP3012) with 3 μg endotoxin-free DS-Red expression plasmid and electroporated using 4D-Nucleofector™ X Unit. Cells were seeded (8×10^5) in 35 mm dishes or plates coated with poly-D-lysine (Sigma-aldrich). Cultures were incubated at 37°C incubator containing 5% CO_2. Twenty-four hours later, the cells were washed with HBSS and the medium was replaced with neuron-specific medium (Neurobasal + 2% of B27, $1 \times$ glutamax, $1 \times$ non-essential amino acids, 50 IU/ml penicillin and streptomycin, Invitrogen).

The medium was changed every 3 days. Recombinant Vpr was added to the culture on days 5 and 7 and neurons were collected or recorded on day 9.

HEK293 (2×10^5) were transfected with 0.5 μg of HIV-1 LTR-luciferase using jetPEI (Polyplus-transfection) for 24 hours and then treated with rVpr (75 or 150 ng/ml) for an additional 24 hours. HEK293 cells treated with 100 ng/ml recombinant HIV-1 Tat protein was used as a positive control. The cells were washed, collected and processed for luciferase assay using the Berthold detection system. Three independent experiments were conducted.

1.3. Live cell image acquisition

Mitochondria transport within the neuronal axons was taken using the 60× oil objective lens of the Leica DMI 4000B confocal microscope. A heated 37°C temperature-controlling chamber filled with 5% CO_2 surrounding the microscope stage was used to keep the cells alive. Images were captured every 5 seconds for a total of 5 minutes. Kymographs were made using ImageJ. Mitochondria moving at a velocity higher than 0.1 μm/s were considered mobile. At least thirty axons were recorded.

1.4. Cytotoxicity assay

Vpr cytotoxicity was measured using Promega CytoTox-Glo kit following the manufacturer's protocol with minor modifications. Briefly, 1×10^5 live cells were plated in each well of a 48-well plate and kept in culture for 8 days. Two hundred microliters of CytoTox-Glo™ reagent was added to all wells, mixed by orbital shaking and then incubated at room temperature for 15 minutes before measuring the luminescence for dead cells. After that, 200 μl of lysis reagent was added to all wells and incubated at room temperature for 15 minutes before measuring total luminescence. Five independent experiments were conducted.

1.5. Cell senescence staining

Senescence was evaluated using β-galactosidase cell staining kit (Cell signaling) as recommended by the manufacturer. Briefly, neurons in 3.5 cm dishes were rinsed, fixed with $1 \times$ fixative solution for 15 minutes, and washed twice with PBS. β-galactosidase staining solution (930 μl $1 \times$ staining solution with 10 μl supplement A, 10 μl supplement B and 50 μl 20 mg/ml X-gal in DMF) was added and the cells were incubated at 37°C without CO_2 overnight. Images were taken with Nikon LED microscope the following day. Experiments were repeated three times.

1.6. ATP assay

ATP content was determined with the ATP Determination Kit (Molecular Probes, Invitrogen) following the manual. Briefly, a standard curve containing ATP concentrations ranging from 1 nM to 1 μM was generated before measuring ATP in the cells. 10 mM carbonyl cyanide m-chlorophenyl hydrazone (CCCP, Sigma-aldrich)-treated neurons were used as a positive control. Cultured neurons were washed in PBS and subject to at least 3 freeze (−80°C) and thaw (37°C) cycles until most of the cell membrane broke.

Total protein concentration was measured using the BCA kit (Pierce) and normalized accordingly. Normalized samples (10 μl) were mixed with 100 μl of standard reaction solution containing DTT, D-luciferin and firefly luciferase. Luminescence was detected with the Berthold detection system. The amount of ATP in the cell samples was calculated from the standard curve. Three independent experiments were conducted.

1.7. Brain slices preparation and immunofluorescence

Old and young mice were decapitated and brains were immediately fixed in 4% paraformaldehyde prepared in PBS. Twenty-four hours later, fixed brains were submerged in 10% sucrose/PBS solution followed by 20% and 30% sucrose until the tissue sank to the bottom of each concentration. Transverse sections of 40 μm were prepared with Leica frozen microtome and kept in PBS. The cells were washed with PBS and fixed with 4% paraformaldehyde in PBS for 20 minutes before staining.

After washing in PBS twice and penetration in PBST (PBS with 0.2% TritonX-100) for 10 minutes (cells) or 20 minutes (brain slices), cells or brain slices were blocked with 2% goat serum for 1 hour at room temperature before incubated with primary antibodies (anti-Tom20, anti-acetyl-α-tubulin 1:100 in 1% goat serum, Santa Cruz) at 4°C overnight. The specimens were washed 4 times, 10 minutes each in PBST. Specimens were then incubated with secondary antibodies coupled with Alex-488 or Alex-594 (1:2000 dilution in PBST, Invitrogen) for 2 hours at room temperature. Specimens were thoroughly washed and mounted in mounting medium with DAPI (Vector Laboratories). The percentage of neurites with inconsecutive distribution of acetyl-α-tubulin was counted half-manually with the Sholl analysis plugin in Image J. Briefly, fluorescent pictures taken with EVOS microscope were converted to 8-bit grayscale pictures and skeletonized with proper threshold settings. Multi-point selection tool was used to mark the total and broken neurites separately. The neurites number can be obtained through Sholl analysis plugin. Percentage of broken neurites would be calculated as broken neurites number/total neurites number. Three independent experiments were conducted.

1.8. Genomic DNA and Methylated DNA Immunoprecipitation (MeDIP)

Genomic DNA was extracted with Thermo Scientific GeneJET Genomic DNA Purification Kit (ThermoFischer) per the manufacturer's protocol. Two micrograms of DNA was sonicated in TE buffer (500 μl) to receive 200–800 bp DNA fragments. Ten microliters of each sample were saved for later use as the input while the rest were boiled for 10 minutes and immediately put on ice. Add 50 μl of 10 × IP buffer (1.4 M NaCl and 0.5% Triton X-100) and incubate with 5 μg 5mC antibody at 4°C overnight. For each sample, wash 50 μl of Dyna beads 3 times with 1 × PBS containing 0.1% BSA followed by one rinse with 1 × IP buffer.

Fifty microliters of Dynabeads were added to each sample and rotated at room temperature for 2 hours. The supernatant was removed with the magnetic rack. Beads were then washed 3 times with 500 μl of 1 × IP buffer and resuspended in 500 μl proteinase K digestion buffer (50 mM Tris pH 8.0, 10 mM EDTA, 0.5% SDS, 10 μl/ml proteinase K) and incubated at 50°C with shaking for 2 hours. One volume phenol/chloroform was then added to the

mixture and centrifuged at the max speed for 5 min at RT. The top layer was transferred to a new tube. After one repeat of the phenol/chloroform extraction, two volumes of cold 100% ethanol, 300 mM NaAc, 2 µg glycogen were added to the mixture and incubated at 4°C overnight. The tubes were centrifuged at 15,000 g for 20 minutes at 4°C and then washed in 70% ethanol. The last procedure was repeated and the DNA was resuspended in appropriate amount of water for PCR analysis.

1.9. Real-time PCR

Total RNA was extracted with TRIzol (Invitrogen) following the manufacturer's protocol and then reverse transcribed into cDNA with the SuperScript VILO cDNA synthesis Kit (Invitrogen). Real-time PCR was performed using SYBR Premix Real-time PCR kit (Roche) per the manufacturer's instruction. The mRNA levels were normalized against β-actin and presented as 2^{-ddCT}. The primer sequences are listed below:

SNCA forward: 5′-ggctttgtcaagaaggaccag-3′, reverse: 5′-cctctgaaggcatttcataagcc-3′

β-actin forward: 5′-ggctgtattcccctccatcg-3′, reverse: 5′-cgtcccagttggtaacaatgcc-3′

PPARGC1α (MeDIP) forward 1: 5′-cagccagatatggacgtaagag-3′, reverse 1: 5′-cacctgtctcaactgctgat-3′;

forward 2: 5′-tcaccctttgttccgtgttatt-3′, reverse 2: 5′-tgcagactcaaactggctatg-3′

1.10. Western Blot Analysis

Cells or tissue were harvested, sonicated and lysed in RIPA buffer (50 mM Tris-HCl, pH 7.5, 150 mM NaCl, 0.5% DOC, 1% NP40, 0.1% SDS, protease inhibitor cocktails), before being centrifuged at 10,000g for 10 minutes at 4°C. Supernatant was collected and protein concentration was measured and normalized using BCA assay kit. BSA was used as the standard. Proteins were separated in 10% sodium dodecyl sulphate-polyacrylamide gel electrophoresis (SDS-PAGE) and transferred to a nitrocellulose membrane (BioRad). Blots were blocked in skim milk and then incubated overnight with primary antibodies: rabbit anti-Miro-1, rabbit anti-GAPDH, rabbit anti-α-synuclein (Cell signaling), mouse anti-Tom 20, or mouse anti-acetyl-α-tubulin (Santa Cruz). Blots were then incubated with secondary antibodies (Invitrogen) conjugated with horseradish peroxidase for 1 hour at room temperature. ECL Plus (Amersham GE Healthcare) was used for detecting the bands. The immunoreactive bands were visualized by autoradiography and the density of the bands was evaluated densitometrically using ImageJ software.

1.11. Statistical Analysis

All experiments were performed at least in triplicates with independent batches of cell cultures. Data were expressed as means ± SEM. Two-group comparisons were analyzed by Student's *t*-test. Multiple comparisons were analyzed by one-way ANOVA followed by the LSD test. *P<0.05, **P<0.01 versus mock group; #P<0.05, ##P<0.01 versus rVpr-treated group.

2. RESULTS

2.1. Mitochondria transport deficiency in aging mice hippocampus

Recent clinical studies identified premature aging or premature age-related comorbidities in HIV-infected patients, suggesting accelerated aging as one of the possible mechanisms contributing to HAND (Capeau, 2011; Holt et al., 2012; Pfefferbaum et al., 2014; Thomas et al., 2013). While abnormal mitochondria axonal transport has been described in neurodegenerative diseases (Calkins et al., 2011; De Vos et al., 2008; Millecamps and Julien, 2013; Perlson et al., 2010; Praprotnik et al., 1996; Trimmer et al., 2009), it remains unclear whether it contributes to the development of HAND. Therefore, we first sought to examine whether mitochondria axonal transport deficiency exists in aging brain.

We used 5- and 18-month-old mice since C57BL/6 mice exhibited aging-related learning and memory deficit from 16 months old (de Fiebre et al., 2006; Liu et al., 2003; Sanders, 2011; Seib et al., 2013). Expression and distribution of the translocase of outer membrane (TOM20) were examined. TOM20 is a protein responsible for the recognition and translocation of cytosolic synthesized mitochondrial pre-proteins (Terada et al., 1997) and commonly accepted as mitochondrial marker. Immunohistochemistry assay revealed more mitochondria accumulation (demonstrated by positive Tom20 staining) in the cell body of hippocampal neurons (CA1 and CA3 areas) of 18-month-old than in the 5-month-old littermates (Figure 1A). We did not observe any difference in the total protein level of Tom20 between the hippocampus of young and aging mice as shown by Western blot analysis (Figure 1B and C). These results suggested that mitochondria accumulation in the hippocampal neurons of 18-month-old mice was probably due to transport deficiency instead of mitochondria quantity changes.

To further verify this hypothesis, we determined the level of several proteins involved in mitochondria axonal transport in young and aging mice. Miro-1 is a Rho-GTPase located in the mitochondria outer membrane and regulates the intracellular microtubule-dependent transport of mitochondria through direct interaction with Milton that recruits the motor proteins (Glater et al., 2006; van Spronsen et al., 2013). Western blot analysis revealed 35.6 % reduction (p<0.05) of Miro-1 in the hippocampus of 18-month-old mice compared to the 5-month-old mice (Figure 1B and C).

Long-range fast axonal transport of mitochondria requires microtubule stabilization (Grafstein and Forman, 1980; Hollenbeck, 1996). Microtubule is the polarized structure composed of heterodimer subunits of α- and β-tubulin (Nogales et al., 1998). Acetylated α-tubulin, present in various microtubule structures, stabilizes the structures of all microtubules (Kim et al., 2012). As shown in panels B and C, the level of acetylated α-tubulin decreased by 37.3% in the hippocampus of 18-month-old mice, suggesting that microtubule stability is compromised in aging brain.

Furthermore, accumulation of α-synuclein has been shown to contribute to microtubule destabilization (Gassowska et al., 2014; Prots et al., 2013), leading to inhibition of mitochondria transport (Xie and Chung, 2012). Therefore, we tested changes in α-synuclein protein level. Using the same protein extracts, we found that α-synuclein expression

increased (2 folds, $p<0.05$) in the hippocampus of 18-month-old compared to the 5-month-old mice (Panels D and E). These data further supported the impairment in mitochondria axonal transport in aging mice hippocampus.

2.2. Determining the optimal dosage of rVpr

Withal the clinical discovery of accelerated aging signs in specific brain regions of HIV patients, the mechanisms, especially the contribution of different viral proteins remain unknown. We therefore wondered whether Vpr caused mitochondria axonal transport deficiency as observed in the aging brains.

We first determined whether the recombinant Vpr was functional. HEK293 cells were transfected with the HIV-1 promoter (LTR) for 24 hours followed by the addition of 75, 150 ng/ml rVpr or 100 ng/ml rTat (used as a positive control). Twenty-four hours later, the cells were washed and processed for luciferase assay. As shown in Figure 2A, rVpr and rTat activated the HIV-1 promoter compared to the untreated.

Vpr has been known to kill cells since it arrests the cell cycle. However, neurons already exit cell cycles and are arrested in a post-mitotic state. In addition, in the cART era, viral replication is under control, allowing low production of viral proteins. We therefore wondered whether low concentration of rVpr can kill neurons or not. An MTT assay was performed to evaluate whether rVpr can affect cell viability in neurons or not. Primary mice neurons were treated with increasing concentration of rVpr (20 – 300 ng/ml) for 48 and 96 hours, respectively. Only 300 ng/ml of rVpr reduced the cell viability by 9% at 96 hours (Figure 2B). No changes were observed when the cells were treated with 150 ng/ml of rVpr for 6 or 24 hours (data not shown).

In addition, we also performed a cytotoxicity assay measuring the activity of protease released from dead cells. Using the CytoTox-Glo kit, we found that 150 ng/ml of rVpr did not induce cytotoxic effect on the cells (panel 2C). Based on these results, 150 ng/ml of rVpr was used in the following experiments.

2.3. rVpr altered mitochondria axonal transport

Next, we examined whether rVpr altered mitochondria axonal transport, hence contributing to the development of early signs of brain aging. Primary mice neurons were transfected with DS-Red expression plasmid. On day 5 post-transfection, the cells were treated with 150 ng/ml of rVpr or heat-inactivated rVpr (H/I rVpr, heated at 100 °C for 10 minutes). A second treatment was performed on day 7. On day 9 post-transfection, the cells were prepared for recording. As shown in Figure 3A and B, rVpr treatment for 4 days reduced the ratio of mobile mitochondria from 29% to 11%. Notice there was no significant difference in the ratio of moving mitochondria in neurons treated with H/I rVpr and untreated, excluding the possible false positive effect brought by protein addition. In comparison, 28-days-old neurons had only 3% mobile mitochondria (panel A). The ratio of moving mitochondria is presented in panel B.

These results demonstrated that instead of causing cell death, low concentration of Vpr impaired mitochondria axonal transport.

2.4. Vpr reduced Miro-1 and disrupted microtubule system

To further confirm the effect of Vpr on mitochondria axonal transport, we examined the protein level of Miro-1 and acetylated α-tubulin in Vpr-treated cells. Mice primary neurons were treated with rVpr for 96 hours after which mitochondrial proteins were collected following the method described by Clayton and Shadel (Clayton and Shadel, 2014). Twenty micrograms of these extracts were subjected to Western blot analysis using anti-Miro-1 and anti-COX IV antibodies. As shown, Miro-1 protein level decreased by 33.94 % ($p<0.01$) in rVpr-treated cells compared to the Mock (panels C and D).

To examine whether Vpr destabilized the microtubule, we performed immunofluorescent assay for acetyl-α-tubulin. In mice, primary neurons, we observed a normal consecutive distribution of acetyl-α-tubulin along the neurites of the untreated cells in contrast to the non-consecutive distribution pattern observed in Vpr-treated cells (panel E). When calculating the percentage of broken neurites, we detected 19.1% of broken neurites (arrow) in Vpr-treated cells compared to only 4% in the untreated cells (panels E and F), suggesting loss of microtubule stability after rVpr treatment. To verify this observation, we performed Tau protein staining and found tau detached from the microtubule and accumulated in the cell body in Vpr-treated cells compared to the untreated (data not shown), further confirming that Vpr disrupted microtubule stability.

2.5. Vpr reduced ATP level in the neurons

We next explored the possible mechanism underlying Vpr-induced mitochondria axonal transport deficiency. Since axonal transport is an energy-dependent process that counts on ATP hydrolysis, we checked intracellular ATP level after Vpr treatment. Primary mice neurons were treated with rVpr for 24, 48 or 96 hours. Cyanide m-chlorophenyl hydrazone (CCCP)-treated neurons were used as a positive control. As shown in Figure 4A, ATP level dramatically decreased in neurons treated with rVpr for 48 (26.64 %, $p<0.01$) and 96 (43.95 %, $p<0.01$) hours respectively but not 24 hours compared to the untreated. These results indicated that Vpr impaired mitochondria axonal transport related with the reduction in ATP.

2.6. Vpr increased protein level of α-synuclein in neurons

Since α-synuclein accumulation is known to impair microtubule stability and contribute to neurological disorders (Jensen et al., 1999), we examined the level of α-synuclein after rVpr treatment. Cytosolic extracts of primary mice neurons treated with 150 ng/ml of rVpr protein for 96 hours were subject to Western blot analysis detected by anti-α-synuclein and anti-GAPDH antibodies. As shown in Figure 4B and C, neurons incubated with rVpr exhibited an increased expression of α-synuclein (3.7 folds over the Mock; $p<0.01$) compared to the untreated.

Therefore, we wondered whether the increase of α-synuclein contributed to the impaired mitochondria axonal transport upon Vpr treatment.

First, we sought to determine the effect of α-synuclein on microtubule stability. Human neuroblastoma cells (SH-SY5Y) were transfected with pcDNA6 empty vector or pcDNA6-

α-synuclein expression plasmid. Transfection rate was almost 100% according to immunofluorescence staining (data not shown). Forty-eight hours post transfection and another 48 hours after cell differentiation the cells were collected and subjected to Western blot analysis. As expected, α-synuclein overexpression resulted in lower acetylated α-tubulin level (Figure 4D, Ac-α-tubulin panel).

It has been shown that α-synuclein protein level increases and becomes more stable with age (Li et al., 2004), which could lead to increased p21[WAF1] level, a senescence marker (Chen et al., 2002). Therefore, we examined the level of p21[WAF1] in α-synuclein-transfected SH-SY5Y cells. As shown in panel D (p21 panel), an increased expression of p21[WAF1] was observed in α-synuclein transfected cells compared to cells transfected with the empty vector. These results confirmed the role of α-synuclein as a deregulator of microtubule stability which mimicked the effect of Vpr. This result also suggested α-synuclein as an inducer of senescence-like phenomenon.

Next, we determined whether the effect of Vpr on acetylated α-tubulin is mediated through α-synuclein. SH-SY5Y cells were transfected with 50 ng of scramble RNA or small RNA inhibitor directed against α-synuclein for 24 hours, differentiated for 48 hours and then treated with 150 ng/ml of rVpr protein for an additional 24 hours. Cells were collected and the total proteins were extracted and subject to Western blot analysis. As shown in Figure 4E, while scramble RNA did not affect the ability of rVpr to induce α-synuclein, rVpr failed to increase the expression of α-synuclein in the presence of siRNA-α-synuclein (lane 3). Consequently, rVpr did not alter the level of acetyl-α-tubulin in the presence of siRNA-α-synuclein (lane 3, α-tubulin panel). This experiment led to the conclusion that Vpr destabilized microtubule through the induction of α-synuclein.

2.7. Bongkrekic acid partially reversed the mitochondria axonal transport deficiency brought by rVpr

Vpr increases the mitochondria membrane permeability (MMP) through interacting with the adenine nucleotide translocator (ANT) via the Arginines in its helical domain III (Sabbah et al., 2006). Meanwhile, it has been shown that bongkrekic acid (BA) can block ANT and reduce MMP, preventing the ATP from leaving the mitochondria (Klingenberg, 2008). Since mitochondria axonal transport is an energy-consuming process that relies on ATP hydrolysis, we examined whether BA could restore the ATP reduction brought by Vpr. Primary neuronal cultures were treated with150 ng/ml rVpr protein alone or with different concentrations of BA. As shown in 5A, addition of 5 μM of BA reversed the ATP reduction caused by Vpr.

Next, we evaluated the effect of BA on mitochondria axonal transport. Neurons transfected with DS-Red expression plasmid were treated with 150 ng/ml of rVpr alone or with 5 μM of BA (Figure 5B). Mitochondria movement was recorded every 5 s for 5 min with the confocal microscope and the spatial position of mitochondria over time was presented as the kymographs. We observed that 5 μM of BA treatment partially restored the ratio of moving mitochondria from 11 % to 21 % in rVpr-treated neurons as compared to the untreated (29 %, $p < 0.05$).

Since 5 μM of BA partially restored the ratio of mobile mitochondria while the same concentration totally reversed the ATP reduction caused by rVpr, we examined whether the same dosage can affect α-synuclein expression in rVpr-treated cells. As expected, rVpr treatment increased the RNA level of α-synuclein RNA as obtained by qPCR assay (Figure 5C). However, 5 μM of BA did not reverse the increase of α-synuclein brought by rVpr (panel C). These results suggest that Vpr deregulated mitochondria axonal transport via multiple mechanisms, ATP reduction caused by Vpr-ANT interaction partially contributed.

2.8. Vpr accelerated the aging process of primary neurons

Cellular dysfunction occurs when non-dividing cells like neurons fail to respond adaptively to age-related environmental stimuli and exhibit premature aging phenotype (Bishop et al., 2010; Mattson and Magnus, 2006). Our data regarding mitochondria axonal transport impairment in rVpr-treated neurons gave us the rationale to determine whether this deficiency explained the premature brain aging observed and described but not fully understood in patients infected with HIV-1.

Therefore, we examined whether Vpr induced aging phenotype in young neurons. Neurons were exposed to rVpr for 96 hours after which the senescence-associated β-galactosidase (SABG) assay was performed. As shown in Figure 6A and B, 16.17 % (p<0.01) of rVpr-treated neurons displayed strong positive staining for X-gal while in the mock group only 3.89 % of neurons were positively stained. This experiment demonstrates that rVpr increased the activity of β-galactosidase, which occurs in old cells.

To further confirm the role of Vpr in inducing aging phenotype in primary neurons, p21^{WAF-1} level was also determined by Western blot, since p21^{WAF-1} is another aging marker as it mediates DNA damage-induced senescence-like phenotype in neurons (Jurk et al., 2012). As shown in panels C and D, treatment of the cells with rVpr led to an increase in p21^{WAF-1} expression by 2.05 folds (p<0.05) as measured by densitometry.

Peroxisome proliferator-activated receptor-gamma coactivator 1 alpha (PGC-1α) is a key transcriptional factor regulating mitochondria biogenesis. Reduction in the PGC-1α expression and function were discovered in aging tissues like skeleton and heart, while interventions like caloric restriction slowed down the aging process associated with the activation of PGC-1α (Anderson and Prolla, 2009; Dillon et al., 2012; Lopez-Lluch et al., 2008). Therefore, we sought to examine PGC-1α changes in rVpr-treated neurons. Using Western blot analysis, we observed decreased PGC-1α protein level (51.87 %, p<0.05) in rVpr-treated cells compared to the untreated (panels C and E).

Aging is known to be associated with epigenetic changes (Brunet and Berger, 2014). We observed an increase in the methylation of the PGC-1α promoter in neurons treated with 75 or 150 ng/ml of rVpr for 48 hours through MeDIP-PCR assay (panel F). This results suggested that Vpr altered PGC-1α expression through increasing DNA methylation in its promoter. Furthermore, histone3 tri-methylated at lysine27 (H3K27Me3) is a repressive epigenetic marker, which drops strikingly with age (Maures et al., 2011). As shown in Figure 6G and H, rVpr reduced the level of H3K27Me3 in neurons (p<0.05). These results further confirmed that Vpr accelerated neuronal aging.

3. DISCUSSION

With the dramatic decrease in HIV-associated dementia but increase in milder forms of neurocognitive disorder in the cART era, understanding neuronal deregulation mechanisms other than apoptosis caused by HIV viral proteins is important for HAND treatment. HIV-1 Vpr has been identified as an HIV accessory protein toxic to neurons through indirect (inflammatory factors released by macrophage and microglia) and direct mechanisms mainly using neuron cell lines instead of primary neurons and mainly apoptosis was proposed as the direct mechanism (Jones et al., 2007). Our lab previously demonstrated that Vpr changed the small non-coding RNA (miRNA) expression profile, contributing to neuronal dysfunctions including deregulation of calcium homeostasis, activation of the oxidative stress, mitochondria dysfunction and v- synaptic retraction (Mukerjee et al., 2011; Rom et al., 2009). In the present study, we treated the mice primary neurons with low concentration of Vpr since viral replication is well under control with the cART treatment. We found while low concentration of Vpr did not induce cell toxicity or death, it impaired mitochondria axonal transport and induced senescence-like phenotype, associated with the signs of pre-mature brain aging observed clinically in HIV patients.

Cellular senescence causes loss of function in neurons and glial cells and is associated with inhibition of neuronal communication, hence contributes to brain dysfunction. Several factors have been shown to affect cell senescence, including diet, high blood pressure, DNA mutations and virus infection (Kukreja et al., 2014; Maillard et al., 2012; Meijers et al., 2013; Murphy et al., 2014; Pfefferbaum et al., 2014). HIV-1 infection has been shown to accelerate senescence in cells deriving from the peripheral immune system, bone, muscle and brain (Cagigi et al., 2013; Erlandson et al., 2013). The molecular and cellular mechanisms underlying the senescence feature caused by HIV-1, as well as which viral protein contributes remain unclear. In the present study, we detected several commonly-accepted senescence markers and demonstrated that HIV-1 Vpr induced cellular senescence-like phenotype in neurons, shedding light on the involvement of senescence in HAND development.

Axonal transport in neurons declines with age (Milde et al., 2015; Takihara et al., 2015). Mitochondria is essential to maintain normal neuronal metabolism and intracellular neuronal communication. Defects in mitochondria axonal transport have been implicated in major neurological diseases such as Alzheimer's disease (Sheng and Cai, 2012). Our data showed mitochondria accumulation in the cell body of hippocampal neurons, together with reduction of Miro-1 and Ac-α-tubulin, strongly supporting the existence of mitochondria axonal transport deficiency in the aging mice brain. Meanwhile, we found Vpr reduced mitochondria axonal transport in neurons, though less potent than colchicine, a microtubule destabilizer (supplementary figure, upper panel). We believed these mitochondria maintained most of the normal functions since we did not observe dramatic changes in Drp1 or phosphor-Drp1, which mediate mitochondria fission, or MCU which is responsible for mitochondria calcium transport. On the other hand, because damaged mitochondria undergo selective mitophagy which is mediated by the accumulation of PINK1 in unhealthy mitochondria (Greene et al., 2012), we also detected PINK1 but did not see any differences between Vpr-treated and untreated neurons (supplementary figure). Therefore, we believe

that low concentration of Vpr affected mitochondria axonal transport without causing massive loss of mitochondria function. Loss of mitochondria supply to the synapses would compromise neuronal communication and the information processing, hence mitochondria axonal transport deficiency might well contribute to the learning and memory deficits often observed in patients living with HIV-1 (Au et al., 2008; Wang et al., 2015).

Further, the generally accepted mitochondria axonal transport model describes on the interaction of two adapter proteins Miro-1 and Milton that link the mitochondria to the motor complexes, which transport the mitochondria along the microtubule system (Glater et al., 2006; van Spronsen et al., 2013). Motor proteins use ATP hydrolysis to power their translocation with the cargoes along microtubule (Hirokawa et al., 2009; Hua et al., 1997; Verhey et al., 2011), whereas decrease in ATP level leads to reduction in mitochondria transport (Miller and Sheetz, 2004). Therefore, compromised mitochondria axonal transport in the presence of Vpr could be attributed to the ATP reduction without major cell death. This is in accordance with an existing research finding ATP depletion by low dosage treatment of sodium azide reversibly inhibited mitochondria axonal transport without causing cell death or axon degeneration (Hirokawa et al., 2009). Depletion of ATP in Vpr-treated cells is not without a precedent. It has been shown that Vpr depleted ATP and caused mitochondria dysfunction in neuro-progenitor cells and impaired neurite outgrowth (Kitayama et al., 2008). Reduction of ATP secretion by Vpr was also seen in astrocytes (Ferrucci et al., 2012). One possible mechanism involved in reduced ATP level is Vpr enters the neurons and binds to the ANT, which exchanges ATP synthesized in the mitochondria for cytosolic ADP (Sabbah et al., 2006).

MPTP blockers such as bongkrekic acid was shown to exert neuroprotective effect against neuronal death caused by ischemia and NMDA-induced excitatory toxicity (Budd et al., 2000; Muranyi and Li, 2005). In the NMDAR-mediated excitotoxicity model, BA binds to ANT, inhibits its permeability, and prevents the drop in mitochondria membrane potential and ATP level which precedes cell death. Similarly, we found BA reduced the loss of ATP caused by Vpr. However, BA treatment only partially reversed mitochondria transport deficiency even though the same dosage could totally reverse ATP loss. This suggested a combination and multi-target treatment promising for the premature aging in HAND.

In addition to reducing energy supply for mitochondria axonal transport, we also found Vpr increased α-synuclein level, which was not related to the Vpr helical domain III that interacts with ANT. Aberrant α-synuclein accumulation has been found in aged substantia nigra neurons, patients with Parkinson's disease, AD or Lewy bodies dementia (Chu and Kordower, 2007; Jellinger, 2004). Further, it has been shown that α-synuclein level increases in the absence of mitochondrial energy and in cells lacking PGC-1α, and high expression of α-synuclein in dorsal root ganglion neurons disrupts the microtubule network (Lee et al., 2006). These publications are in coherent with our data shown in Figures 3 and 5. Our finding that α-synuclein accumulated with age in the hippocampus suggested its involvement in aging. Overexpression of α-synuclein in the SH-SY5Y cells induced the aging markers, further supporting its contribution to age-related learning and memory deficit and its involvement in Vpr-induced accelerated aging. Our study demonstrated for the first time the induction of α-synuclein by Vpr and its contribution to cellular senescence,

suggesting compounds potent to reduce α-synuclein production or accumulation used in combination with BA could be promising for the treatment of HAND.

Unlike resting proliferative cells, post-mitotic neurons have high level of DNMTs. This allows neurons turning ON/OFF activity-regulated genes through DNA methylation changes, leading to synaptic plasticity initiation and long-term memory formation. In our study, neuronal epigenetic pattern reprogramming was found. We believe this epigenetic reprogramming occurs in specific genes since we did not see global genomic methylation level changes with representative measure of methylation in Line-1 repetitive sequences and CCGG sites (data not shown). One of these specific genes was PGC-1α, the reduced expression of which could be explained by loss of CpG methylation at its promoter area. This might be related with the increase of α-synuclein, which was found to bind to the PGC-1α promoter and to contribute to the loss of mitochondrial function (Siddiqui et al., 2012). Our finding is in accordance with existing findings that loss of mitochondria energy disrupts cellular metabolism and DNA methylation, leading to cellular senescence (Hanzelmann et al., 2015; Minocherhomji et al., 2012).

Besides DNA methylation, chromatin marks associated with promoters and gene expression have also shown strong link to neurocognitive and psychiatric disorders (Rando and Simmons, 2015). Ablation of Kmt2a, a histone methyltransferase regulating H3 lysine 4 methylation, was shown to increase anxiety (Shen et al., 2016). On the other hand, loss of EZH2, a histone methyltransferase catalyzing H3 lysine 27 methylation, impaired spatial learning and memory, contextual fear memory and pattern separation (Zhang et al., 2014). Hence, the reduction in H3K27Me3 after Vpr treatment predicted gene expression profile change, which probably led to neurocognitive impairment. Therefore, we concluded that Vpr impaired mitochondria axonal transport and accelerated neuronal senescence via multiple mechanisms including less energy production and α-synuclein increase, with epigenetic regulations involved.

Finally, the experiments were performed *in vitro* and additional *in vivo* studies will be performed in the future to determine the impact of Vpr and/or α-synuclein on mitochondria axonal transport. Further, we previously demonstrated the ability of Vpr mutant (R73S) to overcome the effect of wild-type Vpr (Sawaya et al., 2000). Therefore, using an animal model to determine whether Vpr (injected directly into the hippocampus or delivered using a lentivirus) alters mitochondria axonal transport in the presence of its dominant negative protein will be provide interesting *in vivo* data. Note that Vpr-transgenic mice do not provide a good model to use due to the complications arising from Vpr diffusion into the whole body causing the mice to die shortly after Vpr induction.

In summary, our data showed a novel mechanism through which HIV-1 Vpr accelerated neuronal aging without promoting cell death. These results further explain the persistence of cognitive impairment or HAND (learning deficit and working memory impairment) in HIV patients treated with cART. Intervention in Vpr-induced aberrant protein expression and mitochondria transport deficiency may be a therapeutic target for HAND.

CONCLUSION

Acceleration of normal aging processes and facilitation of age-associated diseases were seen in HIV-infected patients, indicating aging as a probable mechanism underlying HAND. We found Vpr accelerated the aging process of primary neurons, associated with less energy and increase of α-synuclein that inhibited mitochondria axonal transport, as well as hypermethylation of the promoter of one mitochondrial protein. Intervention in Vpr-induced aberrant methylation shift, protein changes and mitochondria transport deficiency may be a therapeutic target for HAND.

Supplementary Material

Refer to Web version on PubMed Central for supplementary material.

Acknowledgments

Abbreviations

Vpr	viral protein R
HAND	HIV-associated neurocognitive disorder
cART	combined anti-retroviral therapy
MPTP	mitochondria permeability transition pore
MMP	mitochondria membrane permeability

References

Anderson R, Prolla T. PGC-1alpha in aging and anti-aging interventions. Biochim Biophys Acta. 2009; 1790:1059–1066. [PubMed: 19371772]

Au A, Cheng C, Chan I, Leung P, Li P, Heaton RK. Subjective memory complaints, mood, and memory deficits among HIV/AIDS patients in Hong Kong. J Clin Exp Neuropsychol. 2008; 30:338–348. [PubMed: 17852611]

Bartlett SE, Reynolds AJ, Hendry IA. Retrograde axonal transport of neurotrophins: differences between neuronal populations and implications for motor neuron disease. Immunol Cell Biol. 1998; 76:419–423. [PubMed: 9797461]

Bartz SR, Rogel ME, Emerman M. Human immunodeficiency virus type 1 cell cycle control: Vpr is cytostatic and mediates G2 accumulation by a mechanism which differs from DNA damage checkpoint control. J Virol. 1996; 70:2324–2331. [PubMed: 8642659]

Bishop NA, Lu T, Yankner BA. Neural mechanisms of ageing and cognitive decline. Nature. 2010; 464:529–535. [PubMed: 20336135]

Borjabad A, Morgello S, Chao W, Kim SY, Brooks AI, Murray J, Potash MJ, Volsky DJ. Significant effects of antiretroviral therapy on global gene expression in brain tissues of patients with HIV-1-associated neurocognitive disorders. PLoS Pathog. 2011; 7:e1002213. [PubMed: 21909266]

Brunet A, Berger SL. Epigenetics of aging and aging-related disease. J Gerontol A Biol Sci Med Sci. 2014; 69(Suppl 1):S17–20. [PubMed: 24833581]

Budd SL, Tenneti L, Lishnak T, Lipton SA. Mitochondrial and extramitochondrial apoptotic signaling pathways in cerebrocortical neurons. Proc Natl Acad Sci U S A. 2000; 97:6161–6166. [PubMed: 10811898]

Cagigi A, Rinaldi S, Santilli V, Mora N, ECM, Cotugno N, Zangari P, Aquilani A, Guzzo I, Dello Strologo L, Rossi P, Palma P. Premature ageing of the immune system relates to increased anti-lymphocyte antibodies (ALA) after an immunization in HIV-1-infected and kidney-transplanted patients. Clin Exp Immunol. 2013; 174:274–280. [PubMed: 23841754]

Calkins MJ, Manczak M, Mao P, Shirendeb U, Reddy PH. Impaired mitochondrial biogenesis, defective axonal transport of mitochondria, abnormal mitochondrial dynamics and synaptic degeneration in a mouse model of Alzheimer's disease. Hum Mol Genet. 2011; 20:4515–4529. [PubMed: 21873260]

Capeau J. Premature Aging and Premature Age-Related Comorbidities in HIV-Infected Patients: Facts and Hypotheses. Clin Infect Dis. 2011; 53:1127–1129. [PubMed: 21998279]

Carey AN, Sypek EI, Singh HD, Kaufman MJ, McLaughlin JP. Expression of HIV-Tat protein is associated with learning and memory deficits in the mouse. Behav Brain Res. 2012; 229:48–56. [PubMed: 22197678]

Chen X, Zhang W, Gao YF, Su XQ, Zhai ZH. Senescence-like changes induced by expression of p21(waf1/Cip1) in NIH3T3 cell line. Cell Res. 2002; 12:229–233. [PubMed: 12296382]

Cheng X, Mukhtar M, Acheampong EA, Srinivasan A, Rafi M, Pomerantz RJ, Parveen Z. HIV-1 Vpr potently induces programmed cell death in the CNS in vivo. DNA Cell Biol. 2007; 26:116–131. [PubMed: 17328670]

Chevalier-Larsen E, Holzbaur EL. Axonal transport and neurodegenerative disease. Biochim Biophys Acta. 2006; 1762:1094–1108. [PubMed: 16730956]

Chu Y, Kordower JH. Age-associated increases of alpha-synuclein in monkeys and humans are associated with nigrostriatal dopamine depletion: Is this the target for Parkinson's disease? Neurobiol Dis. 2007; 25:134–149. [PubMed: 17055279]

Clayton DA, Shadel GS. Purification of mitochondria by sucrose step density gradient centrifugation. Cold Spring Harb Protoc. 2014; 2014 pdb prot080028.

D'Hooge R, Franck F, Mucke L, De Deyn PP. Age-related behavioural deficits in transgenic mice expressing the HIV-1 coat protein gp120. Eur J Neurosci. 1999; 11:4398–4402. [PubMed: 10594667]

de Fiebre NC, Sumien N, Forster MJ, de Fiebre CM. Spatial learning and psychomotor performance of C57BL/6 mice: age sensitivity and reliability of individual differences. Age. 2006; 28:235–253. [PubMed: 22253492]

De Vos KJ, Grierson AJ, Ackerley S, Miller CC. Role of axonal transport in neurodegenerative diseases. Annu Rev Neurosci. 2008; 31:151–173. [PubMed: 18558852]

Dillon LM, Rebelo AP, Moraes CT. The role of PGC-1 coactivators in aging skeletal muscle and heart. IUBMB Life. 2012; 64:231–241. [PubMed: 22279035]

Erlandson KM, Allshouse AA, Jankowski CM, MaWhinney S, Kohrt WM, Campbell TB. Functional impairment is associated with low bone and muscle mass among persons aging with HIV infection. J Acquir Immune Defic Syndr. 2013; 63:209–215. [PubMed: 23392468]

Esteves AR, Gozes I, Cardoso SM. The rescue of microtubule-dependent traffic recovers mitochondrial function in Parkinson's disease. Biochim Biophys Acta. 2014; 1842:7–21. [PubMed: 24120997]

Fellows RP, Byrd DA, Morgello S. Effects of information processing speed on learning, memory, and executive functioning in people living with HIV/AIDS. J Clin Exp Neuropsychol. 2014; 36:806–817. [PubMed: 25111120]

Ferrucci A, Nonnemacher MR, Cohen EA, Wigdahl B. Extracellular human immunodeficiency virus type 1 viral protein R causes reductions in astrocytic ATP and glutathione levels compromising the antioxidant reservoir. Virus Res. 2012; 167:358–369. [PubMed: 22691542]

Forget J, Yao XJ, Mercier J, Cohen EA. Human immunodeficiency virus type 1 vpr protein transactivation function: mechanism and identification of domains involved. J Mol Biol. 1998; 284:915–923. [PubMed: 9837715]

Frederick RL, Shaw JM. Moving mitochondria: establishing distribution of an essential organelle. Traffic. 2007; 8:1668–1675. [PubMed: 17944806]

Gassowska M, Czapski GA, Pajak B, Cieslik M, Lenkiewicz AM, Adamczyk A. Extracellular alpha-synuclein leads to microtubule destabilization via GSK-3beta-dependent Tau phosphorylation in PC12 cells. PLoS ONE. 2014; 9:e94259. [PubMed: 24722055]

Glater EE, Megeath LJ, Stowers RS, Schwarz TL. Axonal transport of mitochondria requires milton to recruit kinesin heavy chain and is light chain independent. J Cell Biol. 2006; 173:545–557. [PubMed: 16717129]

Grafstein B, Forman DS. Intracellular transport in neurons. Physiol Rev. 1980; 60:1167–1283. [PubMed: 6159657]

Greene AW, Grenier K, Aguileta MA, Muise S, Farazifard R, Haque ME, McBride HM, Park DS, Fon EA. Mitochondrial processing peptidase regulates PINK1 processing, import and Parkin recruitment. EMBO Rep. 2012; 13:378–385. [PubMed: 22354088]

Guha D, Nagilla P, Redinger C, Srinivasan A, Schatten GP, Ayyavoo V. Neuronal apoptosis by HIV-1 Vpr: contribution of proinflammatory molecular networks from infected target cells. J Neuroinflammation. 2012; 9:138. [PubMed: 22727020]

Hanzelmann S, Beier F, Gusmao EG, Koch CM, Hummel S, Charapitsa I, Joussen S, Benes V, Brummendorf TH, Reid G, Costa IG, Wagner W. Replicative senescence is associated with nuclear reorganization and with DNA methylation at specific transcription factor binding sites. Clin Epigenetics. 2015; 7:19. [PubMed: 25763115]

He J, Choe S, Walker R, Di Marzio P, Morgan DO, Landau NR. Human immunodeficiency virus type 1 viral protein R (Vpr) arrests cells in the G2 phase of the cell cycle by inhibiting p34cdc2 activity. J Virol. 1995; 69:6705–6711. [PubMed: 7474080]

Heaton RK, Franklin DR, Ellis RJ, McCutchan JA, Letendre SL, Leblanc S, Corkran SH, Duarte NA, Clifford DB, Woods SP, Collier AC, Marra CM, Morgello S, Mindt MR, Taylor MJ, Marcotte TD, Atkinson JH, Wolfson T, Gelman BB, McArthur JC, Simpson DM, Abramson I, Gamst A, Fennema-Notestine C, Jernigan TL, Wong J, Grant I. HIV-associated neurocognitive disorders before and during the era of combination antiretroviral therapy: differences in rates, nature, and predictors. J Neurovirol. 2011; 17:3–16. [PubMed: 21174240]

Heikinheimo T, Poutiainen E, Salonen O, Elovaara I, Ristola M. Three-decade neurological and neurocognitive follow-up of HIV-1-infected patients on best-available antiretroviral therapy in Finland. BMJ Open. 2015; 5:e007986.

Hirokawa N, Noda Y, Tanaka Y, Niwa S. Kinesin superfamily motor proteins and intracellular transport. Nat Rev Mol Cell Biol. 2009; 10:682–696. [PubMed: 19773780]

Hollenbeck PJ. The pattern and mechanism of mitochondrial transport in axons. Front Biosci. 1996; 1:d91–102. [PubMed: 9159217]

Holt JL, Kraft-Terry SD, Chang L. Neuroimaging studies of the aging HIV-1-infected brain. J Neurovirol. 2012; 18:291–302. [PubMed: 22653528]

Hua W, Young EC, Fleming ML, Gelles J. Coupling of kinesin steps to ATP hydrolysis. Nature. 1997; 388:390–393. [PubMed: 9237758]

Jellinger KA. Lewy body-related alpha-synucleinopathy in the aged human brain. J Neural Transm. 2004; 111:1219–1235. [PubMed: 15480835]

Jenkins Y, McEntee M, Weis K, Greene WC. Characterization of HIV-1 vpr nuclear import: analysis of signals and pathways. J Cell Biol. 1998; 143:875–885. [PubMed: 9817747]

Jensen PH, Hager H, Nielsen MS, Hojrup P, Gliemann J, Jakes R. alpha-synuclein binds to Tau and stimulates the protein kinase A-catalyzed tau phosphorylation of serine residues 262 and 356. J Biol Chem. 1999; 274:25481–25489. [PubMed: 10464279]

Jones GJ, Barsby NL, Cohen EA, Holden J, Harris K, Dickie P, Jhamandas J, Power C. HIV-1 Vpr causes neuronal apoptosis and in vivo neurodegeneration. J Neurosci. 2007; 27:3703–3711. [PubMed: 17409234]

Jurk D, Wang C, Miwa S, Maddick M, Korolchuk V, Tsolou A, Gonos ES, Thrasivoulou C, Saffrey MJ, Cameron K, von Zglinicki T. Postmitotic neurons develop a p21-dependent senescence-like phenotype driven by a DNA damage response. Aging Cell. 2012; 11:996–1004. [PubMed: 22882466]

Kim C, Choi H, Jung ES, Lee W, Oh S, Jeon NL, Mook-Jung I. HDAC6 inhibitor blocks amyloid beta-induced impairment of mitochondrial transport in hippocampal neurons. PLoS ONE. 2012; 7:e42983. [PubMed: 22937007]

Kitayama H, Miura Y, Ando Y, Hoshino S, Ishizaka Y, Koyanagi Y. Human immunodeficiency virus type 1 Vpr inhibits axonal outgrowth through induction of mitochondrial dysfunction. J Virol. 2008; 82:2528–2542. [PubMed: 18094160]

Klingenberg M. The ADP and ATP transport in mitochondria and its carrier. Biochim Biophys Acta. 2008; 1778:1978–2021. [PubMed: 18510943]

Koch JC, Bitow F, Haack J, d'Hedouville Z, Zhang JN, Tonges L, Michel U, Oliveira LM, Jovin TM, Liman J, Tatenhorst L, Bahr M, Lingor P. Alpha-Synuclein affects neurite morphology, autophagy, vesicle transport and axonal degeneration in CNS neurons. Cell Death Dis. 2015; 6:e1811. [PubMed: 26158517]

Kukreja L, Kujoth GC, Prolla TA, Van Leuven F, Vassar R. Increased mtDNA mutations with aging promotes amyloid accumulation and brain atrophy in the APP/Ld transgenic mouse model of Alzheimer's disease. Mol Neurodegener. 2014; 9:16. [PubMed: 24885175]

Laguette N, Bregnard C, Hue P, Basbous J, Yatim A, Larroque M, Kirchhoff F, Constantinou A, Sobhian B, Benkirane M. Premature activation of the SLX4 complex by Vpr promotes G2/M arrest and escape from innate immune sensing. Cell. 2014; 156:134–145. [PubMed: 24412650]

Lamberts JT, Hildebrandt EN, Brundin P. Spreading of alpha-synuclein in the face of axonal transport deficits in Parkinson's disease: a speculative synthesis. Neurobiol Dis. 2015; 77:276–283. [PubMed: 25046996]

Lee HJ, Khoshaghideh F, Lee S, Lee SJ. Impairment of microtubule-dependent trafficking by overexpression of alpha-synuclein. Eur J Neurosci. 2006; 24:3153–3162. [PubMed: 17156376]

Li W, Lesuisse C, Xu Y, Troncoso JC, Price DL, Lee MK. Stabilization of alpha-synuclein protein with aging and familial parkinson's disease-linked A53T mutation. J Neurosci. 2004; 24:7400–7409. [PubMed: 15317865]

Liu R, Liu IY, Bi X, Thompson RF, Doctrow SR, Malfroy B, Baudry M. Reversal of age-related learning deficits and brain oxidative stress in mice with superoxide dismutase/catalase mimetics. Proc Natl Acad Sci U S A. 2003; 100:8526–8531. [PubMed: 12815103]

Lopez-Lluch G, Irusta PM, Navas P, de Cabo R. Mitochondrial biogenesis and healthy aging. Exp Gerontol. 2008; 43:813–819. [PubMed: 18662766]

Maday S, Twelvetrees AE, Moughamian AJ, Holzbaur EL. Axonal transport: cargo-specific mechanisms of motility and regulation. Neuron. 2014; 84:292–309. [PubMed: 25374356]

Maillard P, Seshadri S, Beiser A, Himali JJ, Au R, Fletcher E, Carmichael O, Wolf PA, DeCarli C. Effects of systolic blood pressure on white-matter integrity in young adults in the Framingham Heart Study: a cross-sectional study. Lancet Neurol. 2012; 11:1039–1047. [PubMed: 23122892]

Mattson MP, Magnus T. Ageing and neuronal vulnerability. Nat Rev Neurosci. 2006; 7:278–294. [PubMed: 16552414]

Maures TJ, Greer EL, Hauswirth AG, Brunet A. The H3K27 demethylase UTX-1 regulates C. elegans lifespan in a germline-independent, insulin-dependent manner. Aging Cell. 2011; 10:980–990. [PubMed: 21834846]

Meijers RW, Litjens NH, de Wit EA, Langerak AW, van der Spek A, Baan CC, Weimar W, Betjes MG. Cytomegalovirus contributes partly to uraemia-associated premature immunological ageing of the T cell compartment. Clin Exp Immunol. 2013; 174:424–432. [PubMed: 23962178]

Milde S, Adalbert R, Elaman MH, Coleman MP. Axonal transport declines with age in two distinct phases separated by a period of relative stability. Neurobiol Aging. 2015; 36:971–981. [PubMed: 25443288]

Millecamps S, Julien JP. Axonal transport deficits and neurodegenerative diseases. Nat Rev Neurosci. 2013; 14:161–176. [PubMed: 23361386]

Miller KE, Sheetz MP. Axonal mitochondrial transport and potential are correlated. J Cell Sci. 2004; 117:2791–2804. [PubMed: 15150321]

Minocherhomji S, Tollefsbol TO, Singh KK. Mitochondrial regulation of epigenetics and its role in human diseases. Epigenetics. 2012; 7:326–334. [PubMed: 22419065]

Mukerjee R, Chang JR, Del Valle L, Bagashev A, Gayed MM, Lyde RB, Hawkins BJ, Brailoiu E, Cohen E, Power C, Azizi SA, Gelman BB, Sawaya BE. Deregulation of microRNAs by HIV-1 Vpr protein leads to the development of neurocognitive disorders. J Biol Chem. 2011; 286:34976–34985. [PubMed: 21816823]

Muranyi M, Li PA. Bongkrekic acid ameliorates ischemic neuronal death in the cortex by preventing cytochrome c release and inhibiting astrocyte activation. Neurosci Lett. 2005; 384:277–281. [PubMed: 15919152]

Murphy T, Dias GP, Thuret S. Effects of diet on brain plasticity in animal and human studies: mind the gap. Neural Plast. 2014; 2014:563160. [PubMed: 24900924]

Nogales E, Wolf SG, Downing KH. Structure of the alpha beta tubulin dimer by electron crystallography. Nature. 1998; 391:199–203. [PubMed: 9428769]

O'Donnell KC, Lulla A, Stahl MC, Wheat ND, Bronstein JM, Sagasti A. Axon degeneration and PGC-1alpha-mediated protection in a zebrafish model of alpha-synuclein toxicity. Dis Model Mech. 2014; 7:571–582. [PubMed: 24626988]

Perlson E, Maday S, Fu MM, Moughamian AJ, Holzbaur EL. Retrograde axonal transport: pathways to cell death? Trends Neurosci. 2010; 33:335–344. [PubMed: 20434225]

Pfefferbaum A, Rogosa DA, Rosenbloom MJ, Chu W, Sassoon SA, Kemper CA, Deresinski S, Rohlfing T, Zahr NM, Sullivan EV. Accelerated aging of selective brain structures in human immunodeficiency virus infection: a controlled, longitudinal magnetic resonance imaging study. Neurobiol Aging. 2014; 35:1755–1768. [PubMed: 24508219]

Praprotnik D, Smith MA, Richey PL, Vinters HV, Perry G. Filament heterogeneity within the dystrophic neurites of senile plaques suggests blockage of fast axonal transport in Alzheimer's disease. Acta Neuropathol. 1996; 91:226–235. [PubMed: 8834534]

Prots I, Veber V, Brey S, Campioni S, Buder K, Riek R, Bohm KJ, Winner B. alpha-Synuclein oligomers impair neuronal microtubule-kinesin interplay. J Biol Chem. 2013; 288:21742–21754. [PubMed: 23744071]

Rando OJ, Simmons RA. I'm eating for two: parental dietary effects on offspring metabolism. Cell. 2015; 161:93–105. [PubMed: 25815988]

Rom I, Deshmane SL, Mukerjee R, Khalili K, Amini S, Sawaya BE. HIV-1 Vpr deregulates calcium secretion in neural cells. Brain Res. 2009; 1275:81–86. [PubMed: 19328187]

Sabbah EN, Druillennec S, Morellet N, Bouaziz S, Kroemer G, Roques BP. Interaction between the HIV-1 protein Vpr and the adenine nucleotide translocator. Chem Biol Drug Des. 2006; 67:145–154. [PubMed: 16492162]

Sanders MJ. Context processing in aging: older mice are impaired in renewal of extinguished fear. Exp Aging Res. 2011; 37:572–594. [PubMed: 22091582]

Sawaya BE, Khalili K, Gordon J, Srinivasan A, Richardson M, Rappaport J, Amini S. Transdominant activity of human immunodeficiency virus type 1 Vpr with a mutation at residue R73. J Virol. 2000; 74:4877–4881. [PubMed: 10775627]

Schwarz TL. Mitochondrial trafficking in neurons. Cold Spring Harb Perspect Biol. 2013:5.

Seib DR, Corsini NS, Ellwanger K, Plaas C, Mateos A, Pitzer C, Niehrs C, Celikel T, Martin-Villalba A. Loss of Dickkopf-1 restores neurogenesis in old age and counteracts cognitive decline. Cell Stem Cell. 2013; 12:204–214. [PubMed: 23395445]

Shen EY, Jiang Y, Javidfar B, Kassim B, Loh YH, Ma Q, Mitchell AC, Pothula V, Stewart AF, Ernst P, Yao WD, Martin G, Shen L, Jakovcevski M, Akbarian S. Neuronal Deletion of Kmt2a/Mll1 Histone Methyltransferase in Ventral Striatum is Associated with Defective Spike-Timing Dependent Striatal Synaptic Plasticity, Altered Response to Dopaminergic Drugs and Increased Anxiety. Neuropsychopharmacology. 2016; 41:3103–3113. [PubMed: 27485686]

Sheng ZH, Cai Q. Mitochondrial transport in neurons: impact on synaptic homeostasis and neurodegeneration. Nat Rev Neurosci. 2012; 13:77–93. [PubMed: 22218207]

Siddiqui A, Chinta SJ, Mallajosyula JK, Rajagopolan S, Hanson I, Rane A, Melov S, Andersen JK. Selective binding of nuclear alpha-synuclein to the PGC1alpha promoter under conditions of oxidative stress may contribute to losses in mitochondrial function: implications for Parkinson's disease. Free Radic Biol Med. 2012; 53:993–1003. [PubMed: 22705949]

Takihara Y, Inatani M, Eto K, Inoue T, Kreymerman A, Miyake S, Ueno S, Nagaya M, Nakanishi A, Iwao K, Takamura Y, Sakamoto H, Satoh K, Kondo M, Sakamoto T, Goldberg JL, Nabekura J, Tanihara H. In vivo imaging of axonal transport of mitochondria in the diseased and aged mammalian CNS. Proc Natl Acad Sci U S A. 2015; 112:10515–10520. [PubMed: 26240337]

Terada K, Kanazawa M, Yano M, Hanson B, Hoogenraad N, Mori M. Participation of the import receptor Tom20 in protein import into mammalian mitochondria: analyses in vitro and in cultured cells. FEBS Lett. 1997; 403:309–312. [PubMed: 9091323]

Thomas JB, Brier MR, Snyder AZ, Vaida FF, Ances BM. Pathways to neurodegeneration: effects of HIV and aging on resting-state functional connectivity. Neurology. 2013; 80:1186–1193. [PubMed: 23446675]

Trimmer PA, Schwartz KM, Borland MK, De Taboada L, Streeter J, Oron U. Reduced axonal transport in Parkinson's disease cybrid neurites is restored by light therapy. Mol Neurodegener. 2009; 4:26. [PubMed: 19534794]

van Spronsen M, Mikhaylova M, Lipka J, Schlager MA, van den Heuvel DJ, Kuijpers M, Wulf PS, Keijzer N, Demmers J, Kapitein LC, Jaarsma D, Gerritsen HC, Akhmanova A, Hoogenraad CC. TRAK/Milton motor-adaptor proteins steer mitochondrial trafficking to axons and dendrites. Neuron. 2013; 77:485–502. [PubMed: 23395375]

Verhey KJ, Kaul N, Soppina V. Kinesin assembly and movement in cells. Annu Rev Biophys. 2011; 40:267–288. [PubMed: 21332353]

Volpicelli-Daley LA, Gamble KL, Schultheiss CE, Riddle DM, West AB, Lee VM. Formation of alpha-synuclein Lewy neurite-like aggregates in axons impedes the transport of distinct endosomes. Mol Biol Cell. 2014; 25:4010–4023. [PubMed: 25298402]

Wang M, Wang Q, Ding H, Shang H. Association of Hippocampal Magnetic Resonance Imaging With Learning and Memory Deficits in HIV-1-Seropositive Patients. J Acquir Immune Defic Syndr. 2015; 70:436–443. [PubMed: 26258566]

Xie W, Chung KK. Alpha-synuclein impairs normal dynamics of mitochondria in cell and animal models of Parkinson's disease. J Neurochem. 2012; 122:404–414. [PubMed: 22537068]

Zhang J, Ji F, Liu Y, Lei X, Li H, Ji G, Yuan Z, Jiao J. Ezh2 regulates adult hippocampal neurogenesis and memory. J Neurosci. 2014; 34:5184–5199. [PubMed: 24719098]

Zhou D, Wang Y, Tokunaga K, Huang F, Sun B, Yang R. The HIV-1 accessory protein Vpr induces the degradation of the anti-HIV-1 agent APOBEC3G through a VprBP-mediated proteasomal pathway. Virus Res. 2015; 195:25–34. [PubMed: 25200749]

HIGHLIGHTS

HIV-1 Vpr impaired mitochondria axonal transport.

HIV-1 Vpr altered mitochondria axonal transport related to intracellular ATP reduction.

Elevated α-synuclein level also contributed to the effect of Vpr.

Low concentration of HIV-1 Vpr accelerated neuronal aging instead of causing cell death.
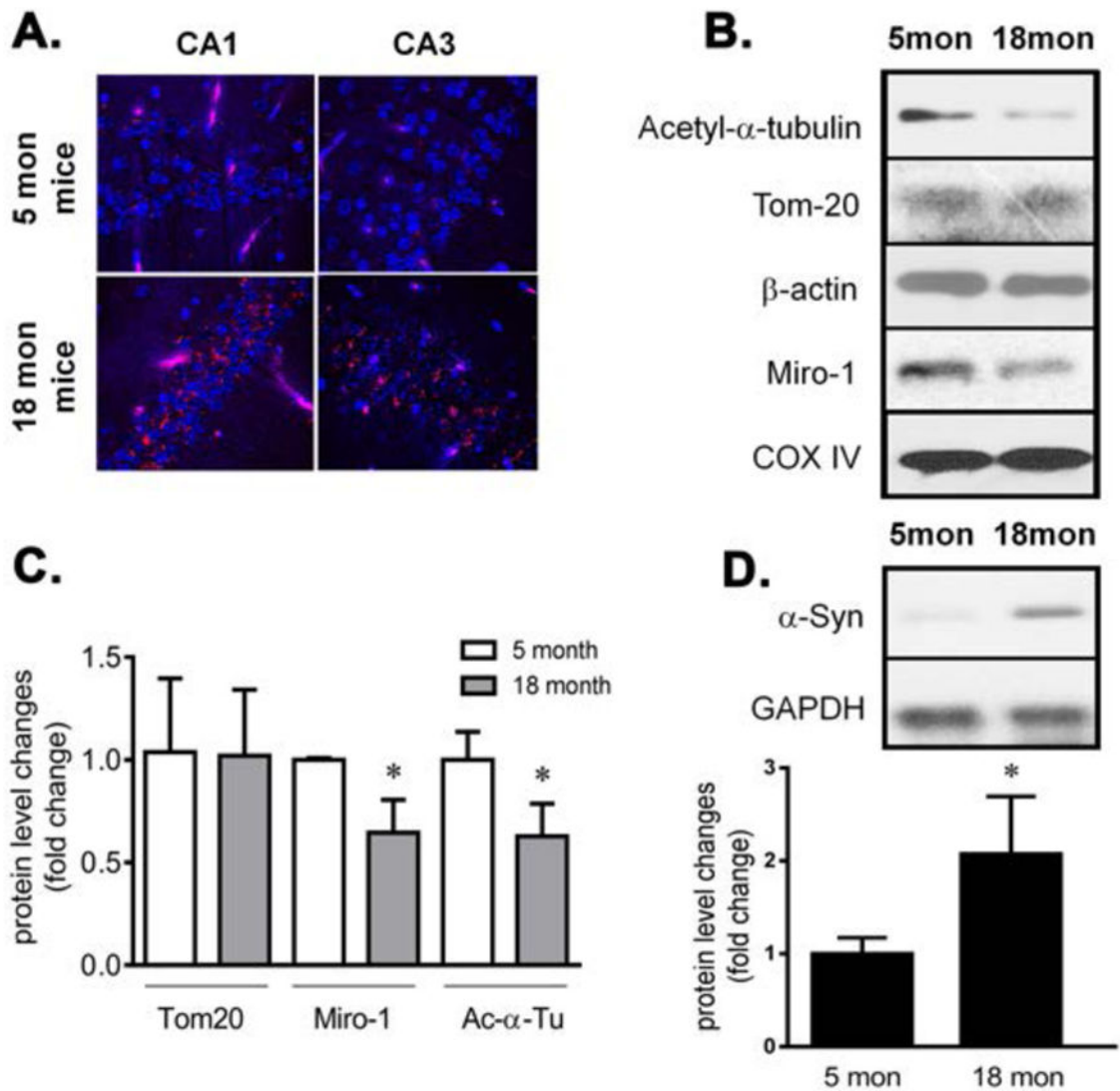
Figure 1. Alteration of mitochondria axonal transport in aging mice
(*A*) Fixed mice hippocampal slides were stained with antibody against Tom20 (red), a mitochondria outer membrane protein used as a mitochondria marker. Mitochondria accumulated around the cell body area (close to the nuclei DAPI) in CA1 and CA3 areas, demonstrating mitochondria transport deficiency. (*B, C*) Reduction in Miro-1 and acetyl-α-tubulin were observed in aging mice hippocampus. No change was observed in Tom-20. β-actin and COX IV were used as loading controls. (*D*) α-synuclein increased in the hippocampus of 18-month-old mice (n = 5).
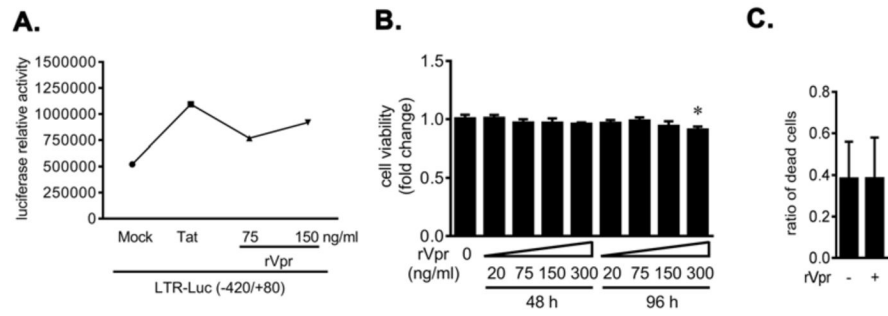
Figure 2. Determining the optimal dosage of rVpr

(*A*) HEK293 cells were transfected with the HIV-1 promoter expression plasmid and then treated with 75 and 150 ng/ml of rVpr or 100 ng/ml of rTat. Luciferase assay was performed and the results are displayed as a histogram. rVpr activated HIV-LTR as rTat did, suggesting the recombinant Vpr was functional. (*B*) MTT assay exhibited no cell viability changes in neurons treated with 20, 75, 150 ng/ml rVpr for 48 or 96 hours compared to the untreated. (*C*) Cytotoxicity assay using primary neurons treated with 150 ng/ml of rVpr. Data is displayed as a histogram. 150 ng/ml of rVpr did not exert cytotoxicity effect on primary neurons. (n=5)
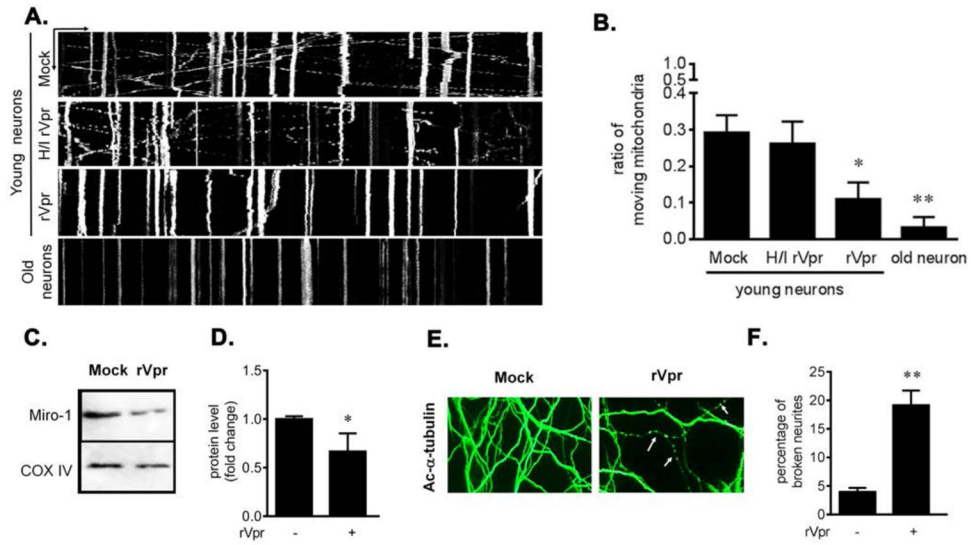
Figure 3. HIV-1 Vpr inhibited mitochondria axonal transport
(*A, B*) Primary neurons were transfected with DS-Red expression plasmid. On days 5 and 7 post transfections the cells were treated with rVpr or heat-inactivated rVpr (H/I). A representative kymograph is shown (*A*) and the percentage of moving mitochondria is displayed as a histogram (*B*). rVpr impaired mitochondria axonal transport. (*C*) 20 μg of protein extracts prepared from mock or from rVpr-treated neurons were subjected to Western blot analysis using anti-Miro-1 antibodies. COX IV was used as a control for equal protein loading. (*D*) Differential protein expression was calculated using densitometry and displayed as a histogram. rVpr reduced Miro-1 level in neurons. (*E, F*) Fluorescence assay showing compromised microtubule stability in rVpr-treated neurons detected by anti-acetyl-α-tubulin. Percentage of broken neurites is displayed as a histogram. Three independent experiments were conducted.
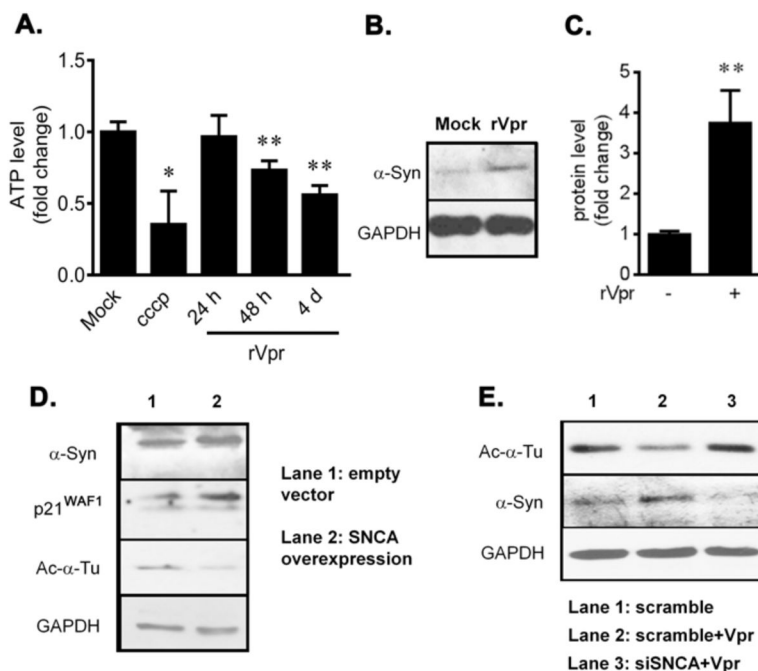
Figure 4. Mechanisms underlying Vpr induced mitochondria axonal transport deficiency

(*A*). Decreased ATP level was observed in primary mice neurons treated with 150 ng/ml of rVpr for 24, 48 or 96 hours or treated with CCCP (used as a positive control). (*B, C*) Protein extracts were prepared from primary mice neurons treated with 150 ng/mL of rVpr for 96 hours. 20 μg of extracts were subjected to Western blot analysis using anti-α-synuclein or -GAPDH (used for equal proteins loading) antibodies. Western blot bands were measured using densitometry and presented as a histogram (C). rVpr increased α-synuclein level in primary neurons. (*D, E*) Protein extracts were prepared from differentiated SH-SY5Y cells transfected with α-synuclein expression plasmid or an empty vector (*D*) or with specific or non-specific siRNA directed against α-synuclein and then treated with 150 ng/mL of rVpr for 24 hours (*E*). 20 μg of extracts were subjected to Western blot analysis using anti-α-synuclein, -p21WAF1, -Ac-α-tubulin or -GAPDH (used for equal protein loading) antibodies as shown in D and F. At least three independent experiments were conducted.
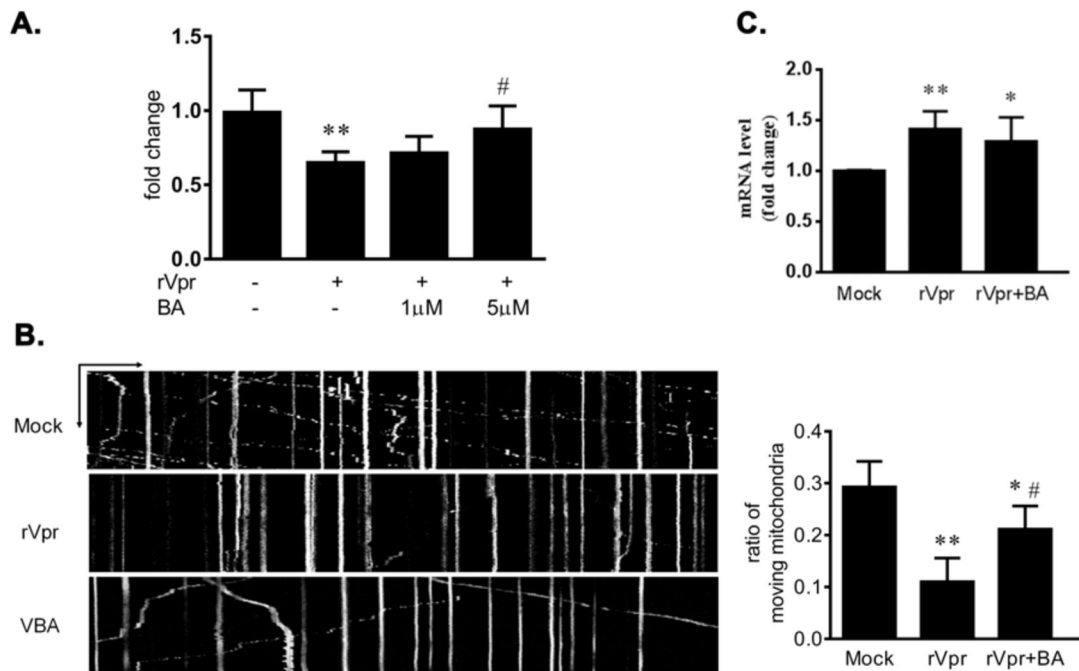
Figure 5. Bongkrekic acid (BA) partially restored the effect of Vpr

(**A**) Primary mice neurons were treated with 150 ng/ml of rVpr alone or along with increasing concentration of BA (1 or 5 μM) for 96 hours. ATP level was measured through luciferase assay and the fold changes is shown as the histogram. 5 μM BA rescued the ATP loss brought by rVpr. (**B**) Kymographs of mitochondria movement in axons of primary neurons (untreated/mock, treated with rVpr or BA+rVpr). Ratio of moving mitochondria compared to the mock is shown as histogram (right panel). 5 μM BA partially restored the percentage of moving mitochondria when co-treated with rVpr. (**C**) SNCA expression was measured by qPCR using total RNA extracted from primary mice neurons treated with rVpr or rVpr + BA. Fold changes are displayed as histograms. 5 μM BA did not affect the increase in SNCA expression caused by rVpr. At least three independent experiments were conducted. **p<0.01 compared to the mock group, #p<0.05 compared to the rVpr group (one-way ANOVA test).
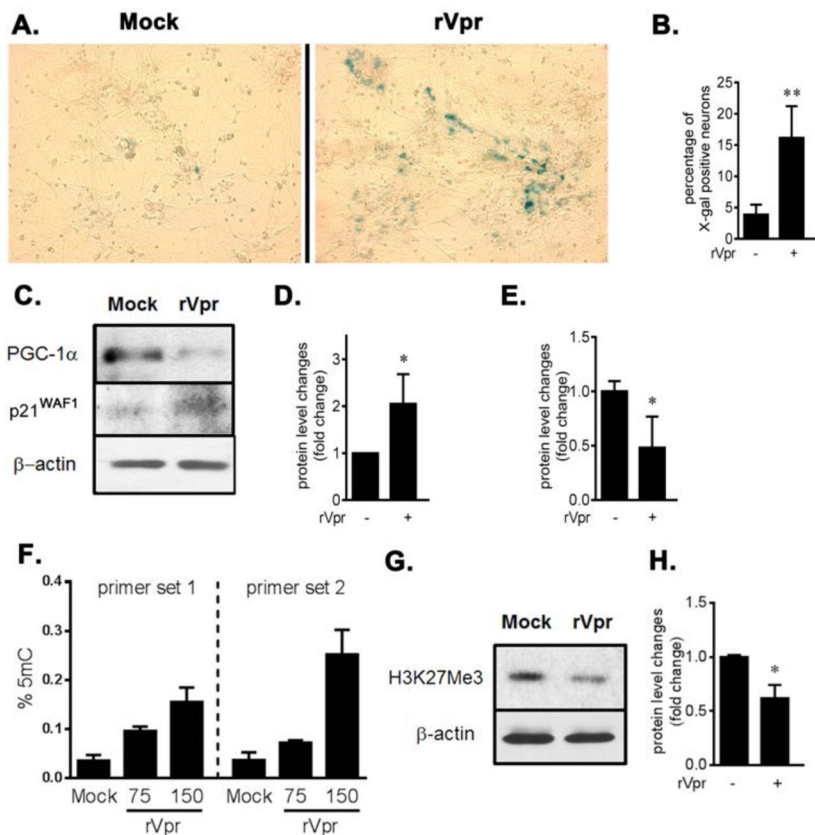
Figure 6. rVpr induced aging phenotype in mice primary neurons

(*A*) Primary mice neurons untreated or treated with 150 ng/ml of rVpr were subjected to β-galactosidase assay using X-gal staining and the percentage of positive stained neurons is displayed in a histogram (*B*). rVpr treatment for 96 hours increased β-galactosidase activity in neurons. (*C – E*) Protein extracts were prepared from primary mice neurons treated with 150 ng/mL of rVpr for 96 hours. 20 μg of extracts were subjected to Western blot analysis using anti-p21^WAF1, -PGC-1α, or -β-actin (used for equal proteins loading) antibodies as shown. Western blot bands were measured using densitometry and presented as a histogram (D and E). Induction of p21^WAF1 and decline in PGC-1α were observed in rVpr-treated neurons. (*F*) Using primary mice neurons, PGC-1α gene promoter methylation was measured using MeDIP assay in neurons treated with 75 or 150 ng/ml of rVpr. 150 ng/ml of rVpr dramatically increased the methylation in PGC-1α gene promoter area. (**G, H**) Protein extracts were prepared from primary mice neurons treated with 150 ng/mL of rVpr for 96 hours. 20 μg of extracts were subjected to Western blot analysis using anti-H3K27me3, or -β-actin (used for equal proteins loading) antibodies as shown. Western blot bands were measured using densitometry and presented as a histogram. Decrease in H3K27me3 was observed in rVpr-treated neurons. (n=4)